Hilton, G. S., Railton, C. J., Ball, G. J., Dean, M., & Hume, A. L. (1997). Modelling a three-element printed dipole antenna array using the FDTD technique. 1062 - 1065. 10.1109/APS.1997.631740

Modelling a Three-Element Printed Dipole Antenna Array using the FDTD Technique.

G.S. Hilton and C.J. Railton
Centre for Communications Research, University of Bristol, Bristol, U.K.

G.J. Ball, M. Dean and A.L. Hume,
DRA, Malvern, U.K.

ABSTRACT.

This paper shows that Finite-Difference Time-Domain (FDTD) analysis incorporating a graded grid may be used to accurately model a three-element triangular array of printed dipoles. Each element forms a complicated structure that combines the microstrip feedline, balun and dipole. Examples of an input response and an element coupling are presented for the range 2GHz - 14GHz, together with far-field radiation patterns for one of the elements at a frequency of 9.3GHz. All the results obtained by the FDTD model run on a low-powered HP 9000 series workstation are compared with measurements of the actual antenna array.

1. ANTENNA ARRAY AND FDTD MODEL.

The Finite-Difference Time-Domain technique is a full-wave numerical method for calculating the electric and magnetic field vectors from Maxwell's curl equations. It has proved to be a suitable technique for the analysis of a single printed dipole antenna [1], and has now been extended in order to determine the characteristics of a triangular array of printed dipoles mounted in front of a reflector.

The array consisted of three antenna elements mounted through rectangular cross-section holes in the reflector. These were placed at the vertices of an equilateral triangle with an 18 mm side, figure 1. For each element, the printed dipole and integrated microstrip balun (based on the design described by Edward and Rees [2]) were fabricated on a 0.64 mm thick alumina dielectric. The microstrip feedline, shown on the upper surface of the dielectric in figure 1, incorporated an open-circuit stub. The 10.0 mm by 0.9 mm dipole and the balanced line feed, seen on the lower dielectric surface, were formed from an extension of the microstrip ground plane.

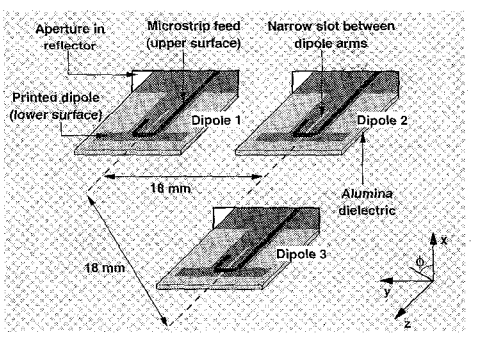

Fig. 1. Layout of the three-element printed dipole array.

0-7803-4178-3/97/$10.00

The FDTD technique required the space immediately surrounding the antenna array to be divided into a number of cells by the use of a three-dimensional Cartesian grid. As this space could not obviously be infinite in size, truncation was performed by the use of wave absorbing boundaries surrounding the whole of the array and feed structure. In the single element model using the same boundary conditions and employing a non-uniform grid [1], the element was modelled using 250000 cells. Again using a similar graded grid, the array had to be modelled with a total of 700000 cells. It should be noted that if a graded grid had not been employed, twice this number of cells would have been required for this model. Only by using a graded grid was it practicable to use just a workstation. The cell sizes varied from 0.5x0.32x0.15mm up to 2.0x2.0x2.0mm. The smallest grid resolution was required in the 0.15mm wide slot between the dipole arms while a coarser grid was employed around the antenna elements. It was therefore the size of the slot that primarily governed the iteration time step of the model, 0.22ps.

The microstrip feedlines for all three antenna elements and the reflector were extended into the absorbing boundaries for the FDTD model. For the feedlines, the boundary represented a good matched termination, while the reflector was regarded by the model as infinite in area since diffraction from the edges of the reflector could not occur. However, for the fabricated antenna array, the feedlines were terminated with (50Ω) SMA connectors, and the reflector used was 180mm square. A further simplification to the model was the non-inclusion of the dielectric loss. Both dielectric loss and diffraction from the reflector edges may be included in the FDTD model, though at the expense of a much larger memory requirement and computer run time.

II. INPUT RESPONSE AND MUTUAL COUPLING.

The FDTD model allows the input response of each antenna element and the mutual coupling between elements to be calculated over a wide frequency band. This was achieved by applying a Gaussian pulse stimulus to the feed of one of the antenna elements, and recording the time-domain voltage responses to this pulse on the microstrip feedlines of all three antennas. The model had to be run for excess of 14000 iterations before the steady-state condition could assume to have been reached. For the fed antenna, the monitored response comprised both the applied pulse and the subsequent reflected wave, whereas for the other two antennas the monitored response was due to coupling alone. The applied and reflected waves were transformed to the frequency domain and processed to produce the input response, while the applied and coupled waves were similarly treated to give the mutual coupling parameters. Using three separate program runs, with a pulse applied to the three array feeds in turn, the input responses for each element S_{11}, S_{22}, S_{33} and the coupled responses S_{12} (=S_{21}), S_{13} (=S_{31}), S_{23} (=S_{32}) were calculated.

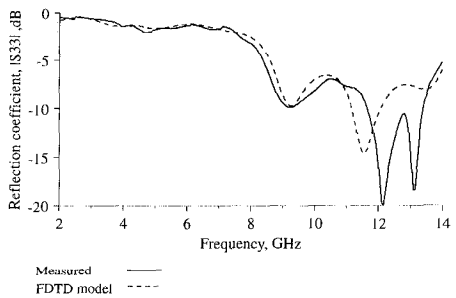

Fig. 2. Input reflection coefficient for dipole 3.

Figure 2 shows the input reflection coefficient as a function of frequency for dipole 3. Very similar responses were obtained for the other two dipoles. It can be seen that there are three

resonances in the frequency range 8-14 GHz, and that there is broad agreement between the measured results and those calculated from the FDTD analysis.

The mutual coupling levels between all the elements of the array were obtained by measurement and FDTD analysis. If the dipole and feed structure had been symmetrical, then only two of the three mutual coupling parameters would have needed to be determined as S_{13} and S_{23} would then have been equal. However, in this case, all three coupling parameters had to be determined since the structure was asymmetrical due to the shape of the microstrip feed. It was found, however, that both the values for S_{13} and S_{23} (calculated and measured) were reasonably close up to about 11 GHz.

The mutual coupling as a function of frequency between dipoles 2 and 3 is shown in figure 3. This example shows that good agreement has been achieved between measurement and analysis, with the maximum measured coupling of -20.5 dB occurring at 9.2 GHz. It can be seen that the measured data contains additional ripple due to the microstrip connector and reflector diffraction effects that were not included in the model.

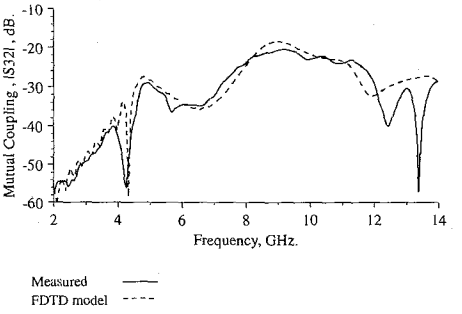

Fig. 3. Mutual coupling between dipole 2 and dipole 3.

III. FAR-FIELD RADIATION PATTERNS.

The far-field radiation patterns were determined for specific frequencies by post-processing stored FDTD near-field data. This involves converting the tangential electric and magnetic field components on five planes surrounding the antenna array, together with their images due to the 'infinite' ground plane, to equivalent current sources. With this information, the far-field electric and magnetic vector potentials can be calculated and then combined to give the far-field radiation levels at any angular direction in space [3].

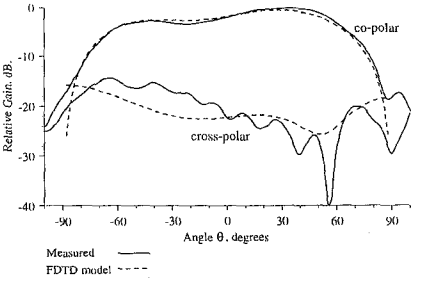

Fig. 4. Far-field H-plane radiation pattern produced by dipole 1 at a frequency of 9.3 GHz.

Figures 4 and 5 show both H-plane (ϕ=0°) and E-plane (ϕ=90°) patterns obtained by measurement and FDTD analysis. In these examples, dipole 1 is fed while the other two elements are terminated with matched loads. Both the co-polar and cross-polar levels are presented for the frequency of 9.3 GHz. It can be seen that the H-plane response has a wider beamwidth and that coupling from the other antenna elements has produced squinted beam patterns for both the planes shown. The measured responses and the analysis are again in good agreement, with the ripple in the measured data and differences in the endfire regions (θ=±90°) being a result of diffraction from the edges of the antenna reflector.

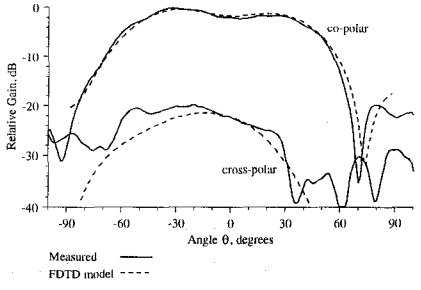

Fig. 5. Far-field E-plane radiation pattern produced by dipole 1 at a frequency of 9.3 GHz.

IV. CONCLUSIONS.

The results presented show how FDTD modelling has been applied to the analysis of complex printed antenna structures with feedline, coupling and radiation effects all automatically included in the model. As well as considering these parameters, the characteristics of various parts of the antenna, such as the balun and dipole, can be investigated by studying the fields in or around such regions. In this way the model has helped to increase the understanding of the operation of the antenna array. The close agreement between the measurement and modelling has meant that there is a very high degree of confidence in using the model to tune the antenna performance. The FDTD technique has now been further developed to allow the prediction of mutual coupling and far-field radiation patterns for larger arrays of elements.

ACKNOWLEDGEMENTS.

This work has been carried out with the support of the Defence Research Agency.

REFERENCES.

[1] G.S. Hilton, C.J. Railton, G.J. Ball, A.L. Hume and M. Dean, "Finite-Difference Time-Domain analysis of a printed dipole antenna" *IEE 9th International Conference on Antennas and Propagation*, pp. 72-75, April 1995.

[2] B. Edward and D. Rees, "A broadband printed dipole with integrated balun", *Microwave Journal*, pp. 339-344, May 1987.

[3] C.A. Balanis, *Antenna Theory*, John Wiley, New York, 1982.